

# Fine-Grained Behavior and Lane Constraints Guided Trajectory Prediction Method

Wenyi Xiong<sup>1</sup>, Jian Chen<sup>2</sup>, *Senior Member, IEEE*, Ziheng Qi<sup>3</sup>

**Abstract**—Trajectory prediction, as a critical component of autonomous driving systems, has attracted the attention of many researchers. Existing prediction algorithms focus on extracting more detailed scene features or selecting more reasonable trajectory destinations. However, in the face of dynamic and evolving future movements of the target vehicle, these algorithms cannot provide a fine-grained and continuous description of future behaviors and lane constraints, which degrades the prediction accuracy. To address this challenge, we present BLNet, a novel dual-stream architecture that synergistically integrates behavioral intention recognition and lane constraint modeling through parallel attention mechanisms. The framework generates fine-grained behavior state queries (capturing spatial-temporal movement patterns) and lane queries (encoding lane topology constraints), supervised by two auxiliary losses, respectively. Subsequently, a two-stage decoder first produces trajectory proposals, then performs point-level refinement by jointly incorporating both the continuity of passed lanes and future motion features. Extensive experiments on two large datasets, nuScenes and Argoverse, show that our network exhibits significant performance gains over existing direct regression and goal-based algorithms.

**Index Terms**—Autonomous driving, dual-stream network, motion prediction, lane attention branch, behavior state attention branch.

## I. INTRODUCTION

THE prediction task has received significant attention from researchers [1]–[3] as an important intermediate step between the perception and decision-making processes. However, the complexity of traffic scenarios (e.g. complex lane constraints and traffic rules) and the uncertainty of the future trajectory modes of vehicles make the forecasting still a major challenge. Today, great success has been achieved in the field of trajectory prediction by utilizing rapidly evolving deep learning techniques. Some frameworks such as Graph Neural Networks (GNN) [4], Convolutional Neural Networks (CNN) [5], etc. are applied to mine the interactions between traffic elements. In addition, the attention mechanism [6] is gradually being widely used by predictive models. Due to its effective modeling of interaction features, the prediction performance is further improved.

Most trajectory prediction networks fall into two categories: direct regression and goal-based methods. Direct regression prediction algorithms [7], [8] focus on extracting multi-agents interactions and complex scene constraints and directly regress to obtain predicted trajectories as show in Fig. 1 (a). For example, HiVT [6] efficiently models the features of a large number of agents in a scene by local context extraction and global interaction modeling, respectively. A reusable multi-context gating fusion module are developed by Multipath++ [9] to extract interaction features and environment features in

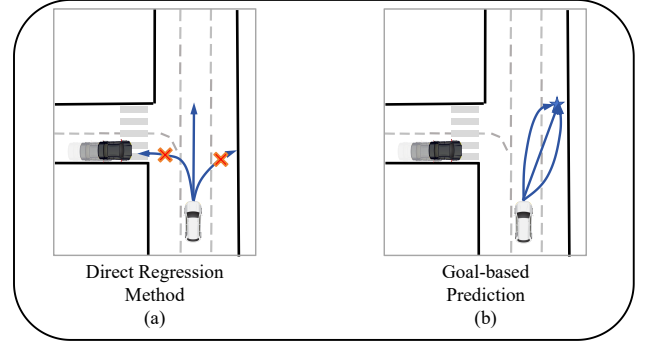


Fig. 1. Illustration of different prediction methods. (a) Direct regression. Unreasonable trajectories may be generated due to the lack of a spatial prior. (b) Goal-based method. There can be different paths to the same goal.

a scene. Although much progress has been made, without the guidance of a spatial prior, it is difficult for such algorithms to accurately predict the multimodality of future trajectories through a single feature-aggregated query, and some implausible future trajectories are thus generated. In order to solve the problem of modal uncertainty, many researchers begin to consider providing priori destinations for prediction, and thus goal-based prediction algorithms emerge as show in Fig. 1 (b). Such algorithms [10]–[12] guide the network to generate a modal-determined trajectory by predicting the possible future destinations or target lanes. The destinations can be manually produced or dynamically predicted by the network. For example, DenseTNT [11] manually produces a large number of target points scattered in the map. However, the performance of prediction depends greatly on the number and quality of candidates. GOHOME [13] utilizes high-definition map graphics and sparse mapping to generate heatmap outputs to predict future target points for final prediction. Ltp [14] predicts the likelihood of each lane segment and from this, trajectories converging to the most probable lane segments are generated and selected. However, the future motion of a vehicle is dynamically changing and is driven by both its own intentions and the structure of the roadway. This leads to the fact that there can be different paths leading to the same goal. Trajectories generated solely from a single destination or a single lane segment tend to ignore detailed spatio-temporal interactions and lane constraints, which degrades model performance.

In order to solve the problems of the two types of methods mentioned above, we propose a novel attention based network as shown in Fig. 2. Inspired by objective factors affecting

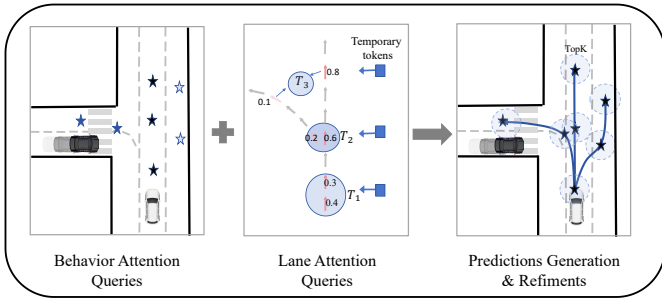


Fig. 2. An overview of the proposed algorithm framework. Unlike existing one token one trajectory (or one goal one trajectory) algorithms, our algorithm utilizes fine-grained behavior queries and lane queries to guide the predictions. Finally, the continuity of the lane and future motion features are aggregated to refine the trajectories at the point-level.

future trajectories, we simultaneously aggregate detailed lane information and driver intent information to predict dynamically evolving target future motions. Specifically, two attention branches are proposed to generate fine-grained behavior state queries and lane queries. The behavior state query reflects the motion intent of the target vehicle at each timestamp under the supervision of the ground truth location. Lane queries aggregate structured lane constraints under the supervision of the lanes that the vehicle will reach in each future timestamp. The two queries are aggregated and fed into a two-stage decoder. The two-stage decoder first predicts future trajectories and further refines the predictions at the point level to make them more reasonable by exploiting the future motion features and the continuity of lane constraints.

Based on the above discussion, our contribution is summarized below:

- We innovatively jointly utilize driving intentions and lane constraints at each timestamp to guide trajectory prediction. In this way, finer-grained scene features are extracted to cope with dynamically evolving vehicle motions and more reasonable trajectories can be obtained.
- A new dual-stream attention network is proposed to acquire behavior state queries and lane queries. Under the supervision of two auxiliary loss functions, these queries are aligned to the vehicle future behaviors and the lane constraints at each timestamps, respectively.
- In the decoder, the future motion and the continuity of lane constraints are further incorporated into the network to achieve point-level trajectory refinement.
- Extensive experimental and ablation studies on two large datasets, NuScenes and Argoverse, show that our algorithm has superior performance compared to existing direct regression methods and goal-based methods.

## II. RELATED WORKS

### A. Scene Feature Modeling

In order to obtain accurate predicted trajectories, it is usually necessary to have a fine-grained modeling of the traffic scenario. CNNs are widely used due to their superior ability to extract localized features. SoPhie [15] utilizes CNN to extract information from scene images. Multi-agent future

interaction relationships and future planning information of controllable vehicles are modeled in PiP [8] using CNN. However, CNNs are limited by their convolutional blocks and ignore the detailed interaction relationships. In order to solve this problem, researchers try to utilize GCNs to obtain a relationship modeling of the nodes in the scene. Grip [4] and Grip++ [16] introduce a static graph and a dynamic graph structure to describe the interactions between transportation agents, respectively. Xu et al. [17] propose a transferable graph neural network that jointly performs motion forecasting and domain alignment. In recent years, transformers have begun to be introduced into the field of trajectory prediction to cope with spatio-temporal information processing. [12], [18]. HiVT [6] divides the problem into attention-based local context extraction and global feature interaction to achieve efficient trajectory prediction results. HPNet [19] models overlapping history frames using the attention mechanism to achieve a multi-frame prediction with continuity. In order to extract more interactions, the common transformer is further extended, e.g., by introducing relative position coding, combining the transformer with graph convolution, etc. [18], [20], [21]. For example, Zhou et al. [22] proposed a new edge-enhanced interaction module to model the relative position information between nodes in the scene. In this paper, we construct a dual-stream attention branches to generate behavior state queries and lane queries at each future timestamp in parallel to guide trajectory prediction.

### B. Direct Regression Prediction Method

This kind of methods [18], [21], [23] mines the interaction features among agents and directly regresses to obtain the final predicted trajectory, as shown in Fig. 1 (a). Many attempts are made to mine more detailed interaction features. For example, Trajectron++ [24] uses a modular graph-structured recursive model to model dynamic interactions in the scene. Hdgt [25] achieves more accurate predictions by modeling the scenario as a heterogeneous graph with different nodes and edges. Simpl [18] designs a symmetric fusion transformer for efficient viewpoint-invariant scene modeling. Zhang et al. [26] explicitly model the edge information between traffic participants, making the network aware of the proximity relationship between them. However, due to the lack of spatial priors, these algorithms converge slowly when faced with multi-modal trajectory prediction. In addition, uncertainty in driving intentions can affect the predictive effectiveness of such algorithms, which in turn can produce some unreasonable predictions. Our algorithm reduces the impact of uncertainty by combining fine-grained behavior state and lane queries to guide predictions.

### C. Goal-Based Prediction Method

This type of approach reduces the complexity of the prediction problem by decomposing the complex trajectory prediction problem into goal regression and trajectory regression, as shown in Fig. 1 (b). In terms of the types of regression destinations, goal-based methods can be categorized into goal-point-based prediction and goal-lane-based prediction.

As pioneers of the goal-point-based approaches, TNT [10] and DenseTNT [11] produce a large number of manual candidate target points. A function is first utilized to predict the probability of each point, and a number of the most likely points are selected to complete the trajectory completion. In order to get rid of a large number of redundant manual goal points for prediction efficiency, algorithms based on adaptive goal points have been proposed. MTR [27] proposes learnable spatial prior queries for simultaneous intent recognition and trajectory refinement. Adapt [12] enhances the accuracy of the endpoint-based prediction algorithm by a gradient-stopping training strategy. The prediction accuracy of such methods depends largely on the quality of the target point. For example, an unreasonable target point can lead to the generation of a trajectory that violates the lane constraints.

Vehicle trajectories on structured lanes are significantly affected by path constraints. Therefore, based on the guidance of a goal lane [14], we can get more reasonable predictions. Inspired by this, PGP [28] explores the trajectory of a vehicle from one lane node to another by training a strategy. Yet such an exploration also comes with a significant computational cost. GOHOME [13] obtains a heat map of the target lanes to guide trajectory prediction and reduce computational cost. Li et al. [29] propose a Dual-Stream Cross Attention to obtain the most likely K target lanes and concatenate them with the target encoding to predict future motion. However, lanes are highly structured and often do not fully reflect fine-grained driver intent, which in turn produces sub-optimal results.

In summary, while goal-based approaches can reduce forecasting uncertainty to some extent, the fact that the future trajectory of a goal is dynamically evolving and is often influenced by both its own intentions and structured lane constraints creates a challenge for forecasting. Thus, our method combine both fine-grained lane constraints and driver behavioral intentions.

### III. PROPOSED MODEL

We propose a novel network framework that utilizes fine-grained behavioral and lane constraints to guide the trajectory predictions as shown in Fig. 3. In the following, we will first introduce the problem setup. Then, we will elaborate on the four components of the network in turn: the encoder, the behavior state attention branch, the lane attention branch, and the two-stage trajectory decoder. Finally, the model training details are introduced.

#### A. Problem Setup

In a traffic scenario, given HD map information and historical observations of traffic participants, the aim of our task is to predict the target future trajectory  $\mathcal{Y} \subseteq \mathbb{R}^{T_f \times 2}$ , where  $T_f$  denotes the prediction time domain. Inspired by Vectornet [7], we vectorize scene elements as shown in Fig. 4 to facilitate prediction networks to encode them to obtain high-dimensional features.

**Map Vectorization:** Specifically, we divide the center-lines of the lanes evenly into  $N_m$  center lane segments, and there are  $S$  lane vectors in each lane segments. From this, we obtain

the map information  $\mathcal{M} \subseteq \mathbb{R}^{N_m \times S \times C_m}$ , where  $C_m$  denotes the feature dimension. Each lane vector contains information about the coordinates of the starting points  $l^s$  and ending points  $l^e$ , the lane attributes  $I_{lane}$  (traffic light, direction, etc.) and the predecessor information  $l^{pre}$  of the starting point. Lane vectors are connected head to tail to form the center line segment. After vectorization, we achieve a computation-friendly representation that retains critical spatial relationships while enabling batched neural network operations.

**Agents Vectorization:** Similar to the processing of map information, we vectorize the historical observation information of agents as  $\mathcal{H} \subseteq \mathbb{R}^{N_v \times T_h \times C_v}$ , where  $N_v$  denotes the number of the agents,  $T_h$  denotes the historical observation time domain, and  $C_v$  denotes the feature channels. For each timestamp, the vector contains information about the coordinates of the starting points  $a^s$  and ending points  $a^e$ , and the agent attribute  $I_{agent}$ .

#### B. Traffic Scene Encoding

We encode the map information  $\mathcal{M}$  and agent historical information  $\mathcal{H}$  that has been vectorized, using RNN and attention. Specifically, the above two types of the information are first mapped to high-dimensional features using two stacked Multi-Layer Perceptrons (MLPs). Subsequently, Gated Recurrent Units (GRUs) are used to aggregate the map and agent history features to obtain  $E_{\mathcal{M}} \subseteq \mathbb{R}^{N_m \times C_e}$  and  $E_{\mathcal{H}} \subseteq \mathbb{R}^{N_v \times C_e}$ , where  $C_e$  denotes the hidden size. Inspired by LaneGCN [30], we input  $E_{\mathcal{M}}$  and  $E_{\mathcal{H}}$  into a fusion architecture to obtain the interaction characteristics between the agent and the map. For the map information, the interaction from agent to lane is computed, and the interaction process can be written as:

$$\hat{E}_{\mathcal{M}} = \mathcal{I}(Q = E_{\mathcal{M}}, K = V = E_{\mathcal{H}}) \quad (1)$$

The specific operation of the interaction process is that we utilize transformer to mine interactions, using map features as queries (Q) and agent features as keys (K) and values (V). The interactive map encodings  $\hat{E}_{\mathcal{M}}$  that aggregate the features of multiple agents are acquired. For agents, similar operations are applied to get the interactive agent encoding  $\hat{E}_{\mathcal{H}}$ :

$$\hat{E}_{\mathcal{H}} = \mathcal{I}(Q = E_{\mathcal{H}}, K = V = \hat{E}_{\mathcal{M}}) \quad (2)$$

In the obtained  $\hat{E}_{\mathcal{H}}$ , we denote the one of the target vehicle as target encoding  $\hat{E}_{tar}$ . We concatenate the acquired map encodings with the agent encodings to get the overall encodings of the scene, denote as  $\hat{E} = \{\hat{E}_{\mathcal{M}}, \hat{E}_{\mathcal{H}}\}$ .

#### C. Behavior State Attention Branch

For traffic participants, their own driving intention is an important factor influencing their future movements [31]. Previous goal-point-based algorithms [11], [12] can reduce the uncertainty of trajectory prediction by providing a goal prior for the prediction, but since trajectories evolve dynamically, there may be different passage paths for the same goal. To address this problem, we propose a behavior state attention branch that provides temporary fine-grained behavioral state

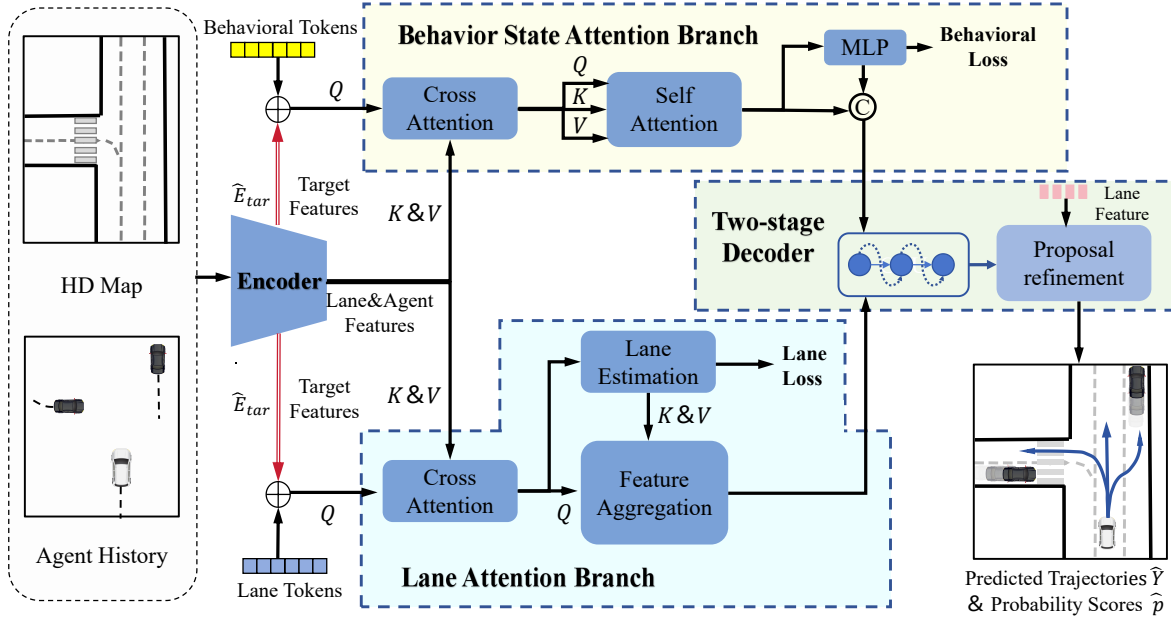


Fig. 3. The pipeline of our proposed algorithm. After vectorization, agent and map information are fed into the encoder and processed using RNN and transformer to get its corresponding high dimensional feature information. Subsequently, we designed two attention branches (lane attention branch and behavior state attention branch) to obtain temporary lane constraints and behavior queries. Finally, a two-stage decoder is designed to predict the target trajectories and refine them at the point-level using the continuity of the lane and future behavior.

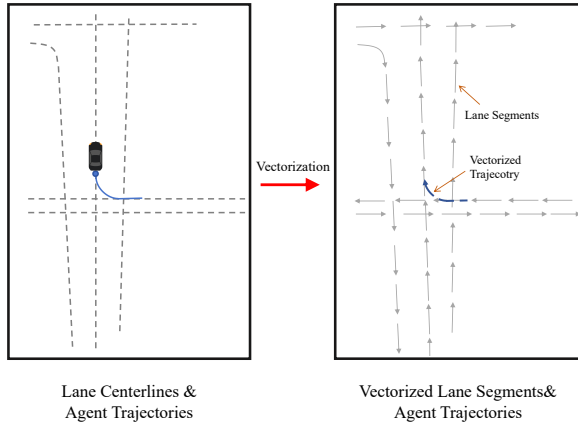


Fig. 4. Scene information vectorization. After vectorization, lane segments and trajectories are represented by a vectors.

priors to guide the prediction. Considering the multi-modal nature of the vehicle’s future trajectory, we assign  $K$  learnable tokens  $B_{tokens}$  to the target coding to obtain the initial behavior queries  $Q_b$ :

$$Q_b = \hat{E}_{tar} + B_{tokens} \quad (3)$$

We use scene encoding  $\hat{E}$  as key and values to perform a cross attention calculation with  $Q_b$  to obtain the interactive features:

$$\hat{Q}_b = \mathcal{I}(Q = Q_b, K = V = \hat{E}) \quad (4)$$

Subsequently, for each interactive behavior query  $\hat{Q}_b$ , interactions between different modalities are parsed utilizing a self-attention module.

$$\hat{Q}_{b,mode} = \mathcal{I}(Q = K = V = \hat{Q}_b) \quad (5)$$

Unlike previous algorithms that only utilize goals to guide predictions, an MLP decodes the behavior queries to initial trajectory proposals  $\hat{\mathcal{Y}}_{coarse} \subseteq \mathbb{R}^{T_f \times K \times 2}$ . We follow the approach of previous algorithms and use a Winner-Takes-All training strategy, an auxiliary  $L_2$  loss  $\mathcal{L}_{behav}$  is used to supervise the quality of the generated initial trajectory proposal:

$$\mathcal{L}_{behav} = \min_{k \in \{1, 2, \dots, K\}} \frac{1}{T_f} \sum_{t=1}^{T_f} \left\| \hat{\mathcal{Y}}_{coarse}^{k,t} - \mathcal{Y}^t \right\|_2^2 \quad (6)$$

where  $\hat{\mathcal{Y}}_{coarse}^k$  denotes  $\hat{\mathcal{Y}}_{coarse}$  for the  $k$ -th modality. Finally, each proposal point is concatenated with the behavior query of its corresponding modality to obtain the final behavior queries  $\hat{Q}_{b,out}$ .

#### D. Lane Attention Branch

For vehicles traveling on structured lanes, their future trajectories are closely related to lane constraints. Trajectories are influenced by different lane information at various moments. In this section, we try to provide fine-grained lane constraints for dynamically evolving trajectories.

First,  $T_f$  learnable tokens  $L_{tokens}$  are assigned to the target encoding  $\hat{E}_{tar}$  to obtain initial lane queries  $Q_L \subseteq \mathbb{R}^{T_f \times C_e}$ :

$$Q_L = \hat{E}_{tar} + L_{tokens} \quad (7)$$

Then, these lane queries are fed into a cross attention module to aggregate comprehensive scene features:

$$\hat{Q}_L = \mathcal{I}(Q = Q_L, K = V = \hat{E}) \quad (8)$$

In the previous sections, we have obtained the encoded information  $\hat{E}_{\mathcal{M}}$  corresponding to each lane segment. We want

each  $\hat{Q}_L$  to aggregate the lane segment features that will be reached at its corresponding future moment. Inspired by [3], [32], a lane scoring module is designed to predict the lane probabilities at each future moment. Specifically, we first treat each  $\hat{Q}_L$  as the key and value, map encoding as queries, and compute the query-lane interaction features  $\mathcal{I}_{\mathcal{L},\mathcal{M}}$ . The  $\mathcal{I}_{\mathcal{L},\mathcal{M}}$ , map encoding, and interactive lane queries are concatenated and fed into an attention mechanism to compute the query-lane scores:

$$S_{\mathcal{L},\mathcal{M}}^{m,t_f} = \frac{\exp(\text{MLP}(\mathcal{I}_{\mathcal{L},\mathcal{M}}^{m,t_f}, \hat{E}_{\mathcal{M}}^m, \hat{Q}_L^{t_f}))}{\sum_{n=1}^{N_m} \exp(\text{MLP}(\mathcal{I}_{\mathcal{L},\mathcal{M}}^{n,t_f}, \hat{E}_{\mathcal{M}}^n, \hat{Q}_L^{t_f}))} \quad (9)$$

where  $S_{\mathcal{L},\mathcal{M}}^{m,t_f}$  denotes the attention score of  $t_f$ -th lane query for the  $m$ -th lane segment. We utilize a binary cross-entropy lane loss to supervise the attention scores:

$$\mathcal{L}_{lane} = \sum_{t_f=1}^{T_f} \mathcal{L}_{CE} \left( S_{\mathcal{L},\mathcal{M}}^{t_f}, S_{GT}^{t_f} \right) \quad (10)$$

where we assign a ground truth label of 1 to the nearest lane segment that the target vehicle arrives at the moment  $t_f$ , and a label of 0 to the rest of the lane segments. We select and concatenate the top  $M$  lane segments features with the  $M$  highest attention scores for each query to obtain  $L_{con}^{t_f}$ :

$$L_{con}^{t_f} = \text{ConCat} \left( \text{top}_M(\hat{E}_{\mathcal{M}}), \text{top}_M(S^{t_f}) \right) \quad (11)$$

where  $\text{top}_M()$  denotes the selection function.  $L_{con}^{t_f}$  are treated as the keys and values to be aggregated into each lane query:

$$\hat{Q}_{lane}^{t_f} = \mathcal{I}(Q = \hat{Q}_L^{t_f}, K = V = L_{con}^{t_f}) \quad (12)$$

Under the supervision of the lane loss, our interactive lane queries are aligned with the lane segments that will be reached at the corresponding future moments, thus effectively guiding the prediction.

### E. Two-stage Decoder

This section presents a two-stage decoder as shown in Fig. 5 (a). In the first stage, it predicts the trajectories of the target vehicles and the modal probabilities. Subsequently, In the second stage, the continuity of the lane constraints and future motion features are utilized to refine the trajectories to obtain the final prediction, the modal probabilities are also updated. For better presentation, a detailed pseudo-code for the two-stage decoder is given in Algorithm 1.

1) *GRU-based predictor*: In the first stage, we predict the target trajectories using a Laplacian mixture density decoder. Unlike previous algorithms [3] that require sampling  $K$  random latent vectors to generate multimodal trajectories, our dual-stream attention branches offer fine-grained  $K \times T_f$  queries based on each target coding to guide multimodal predictions. Specifically, fine-grained queries  $\hat{Q}_{b,out}$  and  $\hat{Q}_{lane}$  from two branches are input into an MLP to get the trajectory feature  $\mathcal{F}_{traj} \subseteq \mathbb{R}^{K \times T_f \times C_{traj}}$ :

$$\mathcal{F}_{traj} = \text{MLP}(\text{Cat}(\hat{Q}_{lane}, \hat{Q}_{b,out})) \quad (13)$$

---

### Algorithm 1: The two-stage decoder

---

**Input:**

$\hat{Q}_{b,out}$ ,  $\hat{Q}_{lane}$ ,  $\hat{E}_{\mathcal{M}}$  and lane segment positions  $P_{\mathcal{M}}$ ;

**Output:**

Predicted trajectories  $\hat{\mathcal{Y}}$  and probabilities  $\hat{P}$ ;

- 1 Aggregate  $\hat{Q}_{b,out}$  and  $\hat{Q}_{lane}$  at  $T_f$  timestamp to predict modal probabilities  $\hat{P}$ .
  - 2 Aggregate  $\hat{Q}_{b,out}$  and  $\hat{Q}_{lane}$  and encode them to obtain future prediction features  $\mathcal{F}_{fut}$  using GRU according to (13) and (14);
  - 3 Decode  $\mathcal{F}_{fut}$  to obtain predicted multimodal proposals  $\hat{\mathcal{Y}}$ , and  $\hat{\mathcal{Y}}_{\mu}$  is the position of the predicted proposals;
  - 4 **if** perform proposals refinement **then**
  - 5     Obtain future motion features  $\mathcal{F}_b$  via (16)
  - 6      $\mathcal{F}'_{Lanecon} \leftarrow \text{Lanecon}(\mathcal{F}_{fut}, \hat{\mathcal{Y}}_{\mu}, \hat{E}_{\mathcal{M}}, P_{\mathcal{M}})$
  - 7     Predict  $\Delta\hat{\mathcal{Y}}_{\mu}$  by aggregating  $\mathcal{F}_b$  and  $\mathcal{F}'_{Lanecon}$
  - 8      $\hat{\mathcal{Y}}_{\mu} \leftarrow \hat{\mathcal{Y}}_{\mu} + \Delta\hat{\mathcal{Y}}_{\mu}$
  - 9     Update  $\hat{P}_{new}$  with  $\mathcal{F}_b$  and  $\mathcal{F}'_{Lanecon}$  at  $T_f$
  - 10     $\hat{P} \leftarrow \hat{P}_{new}$
  - 11    **return**  $\hat{\mathcal{Y}}$  and  $\hat{P}$
  - 12 **end**
  - 13 **else**
  - 14    **return**  $\hat{\mathcal{Y}}$  and  $\hat{P}$
  - 15 **end**
  - 16 **function** Lanecon ( $\mathcal{F}_{fut}, \hat{\mathcal{Y}}_{\mu}, \hat{E}_{\mathcal{M}}, P_{\mathcal{M}}$ ):
  - 17    **for**  $k \leftarrow 1$  **to**  $K$  **do**
  - 18      **for**  $t \leftarrow 1$  **to**  $T_f$  **do**
  - 19         $\text{dist} \leftarrow \|\hat{\mathcal{Y}}_{\mu}^{k,t} - P_{\mathcal{M}}\|_2^2$
  - 20         $\text{idxs} \leftarrow \arg \min^N(\text{dist})$
  - 21         $\hat{E}_{\text{sel}} \leftarrow \hat{E}_{\mathcal{M}}[\text{idxs}]$
  - 22        Aggregate  $\hat{E}_{\text{sel}}$  to obtain  $\mathcal{F}_{lane}^{k,t}$  according to (17)
  - 23      **end**
  - 24    **end**
  - 25    Using GRU to preserve lane continuity to get  $\mathcal{F}'_{Lanecon}$  according to (18).
  - 26    **return**  $\mathcal{F}'_{Lanecon}$
  - 27 **end function**
- 

Then we use the target encoding  $\hat{E}_{tar}$  as the initial hidden state and utilize a GRU to recover future predictions features:

$$\mathcal{F}_{fut} = \text{GRU}(\mathcal{F}_{traj}, h_0 = \hat{E}_{tar}) \quad (14)$$

$\mathcal{F}_{fut}$  are input into two stacked different MLPs to produce the predicted trajectories. Then, we input the  $T_f$ -th lane query and behavior query corresponding to each modality into an MLP to predict the mode probabilities. We denote the result of the proposals as:

$$\hat{\mathcal{Y}} = \sum_{k=1}^K \hat{p}_k \text{Laplace} \left( \hat{\mathcal{Y}}_{\mu}, \hat{\mathcal{Y}}_{\sigma} \right) \quad (15)$$

where  $\hat{p}_k$  denote the predicted probabilities for the  $k$ -th mode, and  $\sum_{k=1}^K \hat{p}_k = 1$ .  $\hat{\mathcal{Y}}_{\mu} \subseteq \mathbb{R}^{T_f \times K \times 2}$  and  $\hat{\mathcal{Y}}_{\sigma} \subseteq \mathbb{R}^{T_f \times K \times 2}$



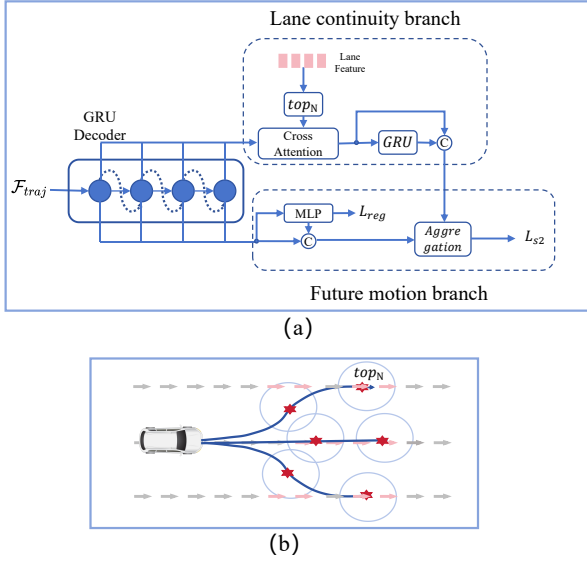


Fig. 5. (a) The two-stage decoder. We first use a simple GRU decoder to predict the target proposals. Subsequently, we use the lane continuity and future behavior to refine the proposals. (b) Illustration of distance-based lane segments selection.

denote the predicted position and scale of each Laplace distribution.

2) *Trajectory refinement*: In the second stage, we try to refine the predictions at the point-level. While fine-grained future behavioral intentions and lane constraints are provided in dual-stream attention networks, the uncertainty of the forecast still exists. This is mainly due to the fact that the prediction results depend heavily on the quality of the predicted lane and behavioral constraints. When the predicted lane constraints from the lane attention branch run counter to the multi-modal behavioral intentions provided by the behavior state attention branch at a certain time, some unreasonable proposals can be produced. To this end, we design a point-level refinement method using the continuity of lane constraints and future motion futures.

Specifically, we first represent future motion features  $\mathcal{F}_b$  by concatenating the corresponding future prediction features with the proposal positions.

$$\mathcal{F}_b^{t_f} = \text{Concat}(\mathcal{F}_{fut}^{t_f}, \hat{\mathcal{Y}}^{t_f}) \quad (16)$$

Inspired by the fact that the lane segments that vehicles travel through are continuous, we try to model the lane continuity into the network. For each trajectory point, we filter and aggregate the nearest  $N$  lane segment features as shown in Fig. 5 (b):

$$\mathcal{F}_{lane}^{k,t} = \mathcal{I} \left( Q = \mathcal{F}_{fut}^{k,t_f}, K = V = \text{top}_N(\hat{E}_{\mathcal{M}}) \right) \quad (17)$$

where  $\mathcal{F}_{lane}^{k,t}$  denotes the aggregated lane feature for trajectory points at moment  $t$  of  $k$ -th mode. Subsequently, we utilize a GRU to encode  $\mathcal{F}_{lane}$  in the temporal dimension to preserve the continuity of the passing lanes:

$$\mathcal{F}'_{Lanecon} = \text{GRU}(\mathcal{F}_{lane}) \quad (18)$$

Finally, future behavioral features  $\mathcal{F}_b$  and lane continuity features  $\mathcal{F}'_{Lanecon}$  are aggregated to predict the proposal deviations  $\Delta\mathcal{Y} = \mathcal{Y} - \hat{\mathcal{Y}}$  between proposals and ground truth. Modal possibilities are also re-predicted, using last-moment future behavioral features combined with lane continuity features.

## F. Model Training

We train the network in two stages. The first stage of the decoder is first trained by minimizing the regression loss  $\mathcal{L}_{reg}$  and classification loss  $\mathcal{L}_{cls}$  of the two auxiliary losses.

$$\mathcal{L}_{s1} = \mathcal{L}_{reg} + \mathcal{L}_{cls} + \lambda_L \mathcal{L}_{lane} + \mathcal{L}_{behav} \quad (19)$$

where  $\lambda_L$  is the lane loss weight. The negative log-likelihood estimation is used to compute regression loss  $\mathcal{L}_{reg}$ . We follow the approach of previous algorithms and use a Winner-Takes-All training strategy to focus on the mode  $k^*$  with the minimum average Euclidean distance to the ground truth among the  $K$  proposals:

$$\mathcal{L}_{reg} = -\frac{1}{T_f} \sum_{t=1}^{T_f} \log P(\mathcal{Y}^t | (\hat{\mathcal{Y}}_{\mu}^{t,k^*}, \hat{\mathcal{Y}}_{\sigma}^{t,k^*})) \quad (20)$$

In addition, inspired by [6], a soft displacement error-based cross-entropy loss is used to compute the classification loss  $\mathcal{L}_{cls}$  for multimodal trajectories:

$$\mathcal{L}_{cls} = -\sum_{k=1}^K p_k \log(\hat{p}_k) \quad (21)$$

where the  $p_k$  denote the target probability.

In the second stage of training, the loss function adds a deviation loss  $\mathcal{L}_d$  and a heading angle loss  $\mathcal{L}_{angle}$  to that of the first stage:

$$\mathcal{L}_{s2} = \mathcal{L}_{s1} + \lambda_d \mathcal{L}_d + \lambda_a \mathcal{L}_{angle} \quad (22)$$

Similar to the first stage of training, we utilize Winner Takes All's strategy to compute the deviation loss and heading angle loss for  $k^*$ -modal proposals:

$$\mathcal{L}_d = \frac{1}{T_f} \sum_{t=1}^{T_f} \left\| \Delta \hat{\mathcal{Y}}^{k^*,t} - \Delta \mathcal{Y}^{k^*,t} \right\|_2^2 \quad (23)$$

$$\mathcal{L}_{angle} = -\frac{1}{T_f} \sum_{t=1}^{T_f} \cos(\hat{\theta}^{k^*,t} - \theta^t) \quad (24)$$

where  $\Delta \hat{\mathcal{Y}}^{k^*,t}$  denotes the predicted deviation for the  $k^*$ -mode.  $\hat{\theta}^{k^*,t}$  and  $\theta^t$  represent the heading angle of the trajectory of the  $k^*$ -mode and the ground truth heading angle at moment  $t$ , respectively.

## IV. EXPERIMENTS

### A. Experiments Setup

1) *Datasets*: We validate the performance of our algorithm on two publicly available large datasets, nuScenes [33] and Argoverse [34].

**Argoverse** motion forecasting dataset contains a variety of compelling scenarios extracted from 1,006 driving hours in Miami and Pittsburgh, totaling 333,441 five-second sequences.

The prediction task involves forecasting the subsequent three-second trajectory of the target agent based on its own trajectory and those of neighboring agents in the initial two seconds. Trajectories are sampled at a rate of 10Hz.

**nuScenes** is a dataset that features a wide array of complex lane scenes captured in urban environments in Boston and Singapore. It includes over 1000 driving scenarios, each lasting 20 seconds and sampled at a frequency of 2Hz. The dataset is primarily focused on the prediction task, where the goal is to forecast 5 trajectories for the upcoming 6 seconds based on observations from the preceding 2 seconds.

2) *Evaluation Metrics*: To evaluate the fit of the multimodal trajectories to the ground truth (GT), we utilize commonly used evaluation metrics:

**Minimum average displacement error** ( $minADE_K$ ): the minimum of the mean L2 distance of the predicted  $k$  multimodal trajectories from GT:

$$minADE_K = \min \left( \frac{1}{T_f} \sum_{t=1}^{T_f} \left\| \hat{\mathcal{Y}}_{\mu}^{t,k} - \mathcal{Y}^t \right\|_2 \right) \quad k = 1, 2, \dots, K \quad (25)$$

**Minimum final displacement error** ( $minFDE_K$ ): the minimum value of the L2 distance between the endpoints of the predicted  $k$  multimodal trajectories and the GT endpoint:

$$minFDE_K = \min \left( \left\| \hat{\mathcal{Y}}_{\mu}^{T_f,k} - \mathcal{Y}^{T_f} \right\|_2 \right) \quad k = 1, 2, \dots, K \quad (26)$$

When  $K = 1$  in the above evaluation metrics, it indicates the calculation of ADE and FDE for the most likely trajectories.

**Brier minimum Final Displacement Error** ( $b - minFDE_K$ ): This metric is similar to  $minFDE_K$ , but additional  $(1.0 - \hat{p}_K)^2$  is added to the endpoint loss.

## B. Quantitative Analysis

In this section, we quantitatively compare the performance of the proposed model with other state-of-the-art algorithms.

1) *Comparison with State-of-the-Arts in NuScenes*: The evaluation performance of our algorithm on the Nusences dataset against other state-of-the-art algorithms is displayed in Table I. We categorize these proposed methods into direct regression algorithms and goal-based algorithms. Direct regression algorithms include CoverNet [35], Trajectron++ [36], Autobot [37], and ContextVAE [38]. They improve prediction accuracy by extracting finer scene features. For example, ContextVAE [38] employs a dual attention mechanism that integrates environmental context from semantic maps and dynamic agents' social interactions. However, these algorithms are heavily influenced by the uncertainty of the trajectory modality, which in turn generates some sub-optimal results. Goal-based methods include Lapred [39], GOHOME [13], TOMAS [40], PGP [28], G2LTraj [41] and Efficient [29]. They mitigate prediction uncertainty by destination and target lane guidance. For example, Efficient [29] selects  $K$  possible goal lanes to guide the multimodal trajectories generations. But these algorithms also have limitations due to the dynamics

of future trajectories. Our method advances trajectory prediction by jointly leveraging fine-grained lane topology queries and intention-aware behavior queries, which collaboratively constrain the multi-modal prediction space. This dual-query mechanism enables the model to achieve state-of-the-art performance, with remarkable metrics of  $minADE_5=1.16$  and  $minFDE_1=6.67$ . Compared with Efficient [29] - the recently proposed method - our framework demonstrates significant improvements of 13.4% and 10.2% in these respective metrics.

2) *Comparison with State-of-the-Arts in Argoverse*: To better demonstrate the generalization performance of our algorithm, we further give a performance comparison with other state-of-the-art algorithms on the Argoverse dataset as shown in Table. II. Similarly, we categorize the methods into direct regression and goal-based algorithms. In this leaderboard, direct regression algorithms include LaneGCN [30], HiVT [6], SceneTrans [42], Multipath++ [9], Q-EANet [43], and Simpl [18], while goal-based algorithms include LTP [14], PBP [44], and Adapt [12]. We find that our algorithm still remains competitive compared to the above mentioned algorithms, and achieves  $minADE_6$  of 0.75,  $minFDE_6$  of 1.11, and  $b-minFDE_6$  of 1.78. Compared to the recently proposed Simpl, our algorithm drops more than 5% in both  $minADE_6$  and  $minFDE_6$ . This demonstrates that our network can exhibit good generalization over different datasets using fine-grained queries.

## C. Ablation Study

In order to analyze the contribution of each network module and determine the optimal network structure, we conduct extensive ablation experiments.

1) *Contribution of each network component*: The prediction performance of different network variants is summarized in Table III, which systematically demonstrates the contribution of each component to the overall framework.

**1. Baseline with Encoder Features (Row 1)**: Using encoder features alone generates rough predictions due to the lack of the guidance of the priors.

**2. Behavior State Attention Branch (Row 2)**: Incorporating the behavior state attention branch introduces fine-grained driving intentions, therefore the prediction accuracy is boosted.

**3. Lane Attention Branch (Row 4)**: The introduction of the lane attention branch further brings fine-grained lane constraints at each moment to the network to jointly guide the prediction and improve the prediction performance.

**4. Decoder Design Comparison (Row 3)**: Replacing the GRU decoder with an LSTM leads to suboptimal results, indicating that GRU's simpler architecture is more effective for trajectory decoding in this framework.

### 5. Refinement Module (Rows 5-6):

- Adding future motion refinement (Row 5) reduces the  $minFDE$  metric (especially for  $minFDE_1$ ) by aligning predictions with intent-aware features.
- Further integration of the lane continuity constraint (Row 6) ensures the continuity of the trajectory, which in turn leads to the optimization of all evaluation metrics.

TABLE I  
COMPARISON WITH OTHER STATE OF THE ART ALGORITHMS IN THE NUSCENCES DATASET LEADERBOARD

Method Types	Models	Year	minFDE <sub>1</sub>	minADE <sub>5</sub>	minFDE <sub>5</sub>	minADE <sub>10</sub>	minFDE <sub>10</sub>
Direct Regression	CoverNet [35]	2020	9.26	1.96	-	1.48	-
	Trajectron++ [36]	2020	9.52	1.88	-	1.51	-
	AutoBot [37]	2022	8.19	1.37	-	1.03	-
	ContextVAE [38]	2023	8.24	1.59	3.28	-	-
Goal-based Method	Lapred [39]	2021	8.12	1.53	3.37	1.12	2.39
	GOHOME [13]	2022	6.99	1.42	-	1.15	-
	TOMAS [40]	2022	6.71	1.33	-	1.04	-
	PGP [28]	2021	7.17	1.27	2.47	0.94	1.55
	G2LTraj [41]	2024	8.30	1.40	-	0.96	-
	Efficient [29]	2024	7.43	1.34	-	-	-
Fine-grained Queries	<b>Our Method</b>	-	<b>6.67</b>	<b>1.16</b>	<b>2.18</b>	<b>0.91</b>	<b>1.44</b>

TABLE II  
COMPARISON WITH OTHER STATE OF THE ART ALGORITHMS IN THE ARGOVERSE DATASET LEADERBOARD

Method Type	Model	Year	minADE <sub>6</sub>	minFDE <sub>6</sub>	b-minFDE <sub>6</sub>
Direct Regression	LaneGCN [30]	2020	0.87	1.36	2.05
	HiVT [6]	2022	0.77	1.17	1.84
	SceneTrans [42]	2022	0.80	1.23	1.89
	Multipath++ [9]	2022	0.79	1.21	1.79
	Q-EANet [43]	2024	0.80	1.23	1.92
	SimpL [18]	2024	0.79	1.18	1.81
Goal-based Method	LTP [14]	2022	0.83	1.30	1.86
	PBP [44]	2023	0.86	1.33	1.98
	Adapt [12]	2023	0.79	1.17	1.80
Fine-grained Queries	<b>Our Method</b>	-	<b>0.75</b>	<b>1.11</b>	<b>1.78</b>

2) *Impact of different numbers of lane segments:* In the Lane Attention Branch, top  $M$  lane segments with the highest probability scores are selected. We explore the effect of different number of lane segments  $M$ . Table IV shows the performance of our network with different number of lane segments  $M = \{1, 2, 3, 4\}$ . It can be seen that  $M = 2$  achieves peak performance in multimodal-trajectory prediction (minADE<sub>5</sub>: 1.17, minFDE<sub>5</sub>: 2.26), while  $M = 1$  attains the lowest minFDE<sub>1</sub>. Notably, further increasing  $M$  to 4 yields stagnant performance with marginally higher minFDE<sub>1</sub>. This suggests that moderate lane selection ( $M = 2$ ) optimally balances feature sufficiency, whereas excessive segments ( $M \geq 3$ ) introduce redundant features without predictive benefits.

Similarly, in the Trajectory Refinement, nearest  $N$  lane segment features are selected for each trajectory point. From the prediction results in Table V, we can conclude that selecting the nearest  $N = 2$  lane segments yields optimal prediction performance across all metrics. While increasing  $N$  from 1 to 2 improves trajectory precision, further expansion to  $N \geq 3$  introduces redundant lane features that dilute the model’s focus, resulting in consistent performance degradation.

3) *Effect of fine-grained queries:* In contrast to previous algorithms that used only the goal prior to guide the entire trajectory prediction, our algorithm employs fine-grained queries. Therefore, we further explore the advantages of our proposed method, as shown in the Table VI. For a fair comparison, predictions guided by both fine-grained queries and only goal queries are not refined. It can be seen that the fine-grained queries achieve improvements over goal-based queries, with

lower prediction errors across all key metrics ( $minFDE_1$ ,  $minADE_5$ ,  $minFDE_5$ ). This highlights the effectiveness of fine-grained queries in capturing nuanced spatial-temporal details, enabling more precise trajectory predictions.

4) *Effect of the lane continuity:* We explicitly model lane segment continuity in multimodal trajectory prediction using GRU networks, ensuring temporal coherence between connected lane segments. In contrast, the baseline method simply aggregates the nearest  $K$  lane segments at each trajectory point without preserving continuity relationships. As shown in Table VII, our continuity-aware approach achieves 2.2% ( $minFDE_1$ ) and 1.8% ( $minFDE_5$ ) performance gains over the baseline, demonstrating that encoding lane topology significantly enhances trajectory precision.

#### D. Qualitative Analysis

To intuitively validate our algorithm’s capabilities, we conduct trajectory visualizations using diverse traffic scenarios from the NuScenes validation set, as illustrated in Fig. 6. The predicted multi-modal trajectories (green lines) closely mirror the ground-truth trajectories (red lines) across critical driving maneuvers: during straight movements (including both unobstructed cruising and slow driving patterns in traffic jams), left turns and right turns (in both urban crossings and controlled channelized lanes). Notably, the trajectories exhibit geometrically coherent curvature transitions (e.g., smooth arc alignment matching lane geometry during dedicated-lane turns) and maintain direction consistency (e.g., stable heading angles in straight paths despite adjacent lane distractions), while dynamically adapting speed profiles (arrow density variations) to scenario-specific constraints like slow driving in congested flows. These visual comparisons confirm the algorithm’s robust generalization in capturing both intent diversity (simultaneously predicting lane-keeping and turning options) and kinematic realism across heterogeneous lane structures.

#### E. Model Complexity Analysis

In table VIII, we analyze the computational cost of our proposed algorithm. Our method achieves the best  $minFDE_6$  performance (1.11) compared to existing approaches, demonstrating superior prediction accuracy. Although our inference time is slightly higher than SimpL (12 ms) and HiVT (20 ms),



TABLE III  
ABLATION STUDY OF NETWORK COMPONENTS

Encoder	Behavior State Attention	Lane Attention	Decoder Type	Refinement		minFDE <sub>1</sub>	minADE <sub>5</sub>	minFDE <sub>5</sub>
				Future Motion	Lane Continuity			
✓	–	–	GRU	–	–	7.52	1.26	2.50
✓	✓	–	GRU	–	–	7.28	1.21	2.36
✓	✓	✓	LSTM	–	–	7.12	1.19	2.31
✓	✓	✓	GRU	–	–	6.99	1.17	2.26
✓	✓	✓	GRU	✓	–	6.84	1.17	2.23
✓	✓	✓	GRU	✓	✓	<b>6.67</b>	<b>1.16</b>	<b>2.18</b>

TABLE IV  
ABLATION STUDY ON THE NUMBER OF MOST PROBABLE LANE SEGMENTS  $M$

The number of the Selected Lane Segments $M$	minFDE <sub>1</sub>	minADE <sub>5</sub>	minFDE <sub>5</sub>
1	<b>6.90</b>	1.18	2.27
2	6.99	<b>1.17</b>	<b>2.26</b>
3	7.01	1.18	2.27
4	7.00	1.18	2.27

TABLE V  
ABLATION STUDY ON THE NUMBER OF NEAREST LINE SEGMENT  $N$

The number of the Selected Lane Segments $N$	minFDE <sub>1</sub>	minADE <sub>5</sub>	minFDE <sub>5</sub>
1	6.83	1.16	2.18
2	<b>6.67</b>	<b>1.16</b>	<b>2.18</b>
3	6.92	1.17	2.21
4	6.93	1.17	2.21

it is still within the practical range for real-world applications. Notably, our model strikes a good balance between efficiency and performance: it requires only 0.60 GFLOPs - considerably less than SimplL, and comparable to HiVT - and uses 2.21M parameters, which is close to the HiVT and far less than LaneGCN. These results highlight that our approach achieves state-of-the-art prediction accuracy at an acceptable computational cost, making its deployment in autonomous systems both effective and efficient.

TABLE VI  
ABLATION STUDY ON FINE-GRAINED QUERIES

Query Type	minFDE <sub>1</sub>	minADE <sub>5</sub>	minFDE <sub>5</sub>
Goal-based queries	7.08	1.20	2.30
Fine-grained queries	<b>6.99</b>	<b>1.17</b>	<b>2.26</b>

TABLE VII  
ABLATION STUDY ON DUAL-ATTENTION BRANCHES

Lane Continuity	minFDE <sub>1</sub>	minADE <sub>5</sub>	minFDE <sub>5</sub>
–	6.82	1.16	2.22
✓	<b>6.67</b>	1.16	<b>2.18</b>

TABLE VIII  
COMPARISON OF COMPUTATIONAL COSTS WITH OTHER ALGORITHMS

Method	minFDE <sub>6</sub>	Inference Time (ms)	FLOPs (G)	Parameters (M)
LaneGCN [30]	1.36	23	1.30	3.68
SimplL [18]	1.18	<b>12</b>	6.70	<b>1.56</b>
HiVT [6]	1.17	20	<b>0.14</b>	2.28
Our method	<b>1.11</b>	30	0.60	2.21

## F. Conclusion

In this study, we propose a novel trajectory prediction framework that systematically integrates fine-grained lane constraints with behavioral patterns through a dual-stream attention architecture. The proposed model features two complementary components: a lane attention branch dedicated to extracting detailed lane topology features, and a behavior state attention branch specialized in capturing driving intention representations. We further enhance prediction accuracy by employing a two-stage decoding mechanism, where initial trajectory proposals are first generated and subsequently refined by incorporating lane continuity and behavioral pattern constraints into the network. Experimental evaluations demonstrate that our framework achieves state-of-the-art performance on both NuScenes and Argoverse benchmarks, with comprehensive ablation studies confirming the individual contributions of each proposed module. Future research will focus on developing an adaptive fusion architecture that dynamically balances the quantitative influences of environmental constraints and agent behaviors, thereby enabling more principled trajectory prediction through explicit interaction modeling.

## REFERENCES

- [1] X. Chen, H. Zhang, F. Zhao, Y. Cai, H. Wang, and Q. Ye, "Vehicle trajectory prediction based on intention-aware non-autoregressive transformer with multi-attention learning for internet of vehicles," *IEEE Transactions on Instrumentation and Measurement*, vol. 71, pp. 1–12, 2022.
- [2] H. Guo, Q. Meng, D. Cao, H. Chen, J. Liu, and B. Shang, "Vehicle trajectory prediction method coupled with ego vehicle motion trend under dual attention mechanism," *IEEE Transactions on Instrumentation and Measurement*, vol. 71, pp. 1–16, 2022.
- [3] M. Liu, H. Cheng, L. Chen, H. Broszio, J. Li, R. Zhao, M. Sester, and M. Y. Yang, "Laformer: Trajectory prediction for autonomous driving with lane-aware scene constraints," in *Proceedings of the IEEE/CVF Conference on Computer Vision and Pattern Recognition*, 2024, pp. 2039–2049.
- [4] X. Li, X. Ying, and M. C. Chuah, "Grip: Graph-based interaction-aware trajectory prediction," in *2019 IEEE Intelligent Transportation Systems Conference (ITSC)*. IEEE, 2019, pp. 3960–3966.

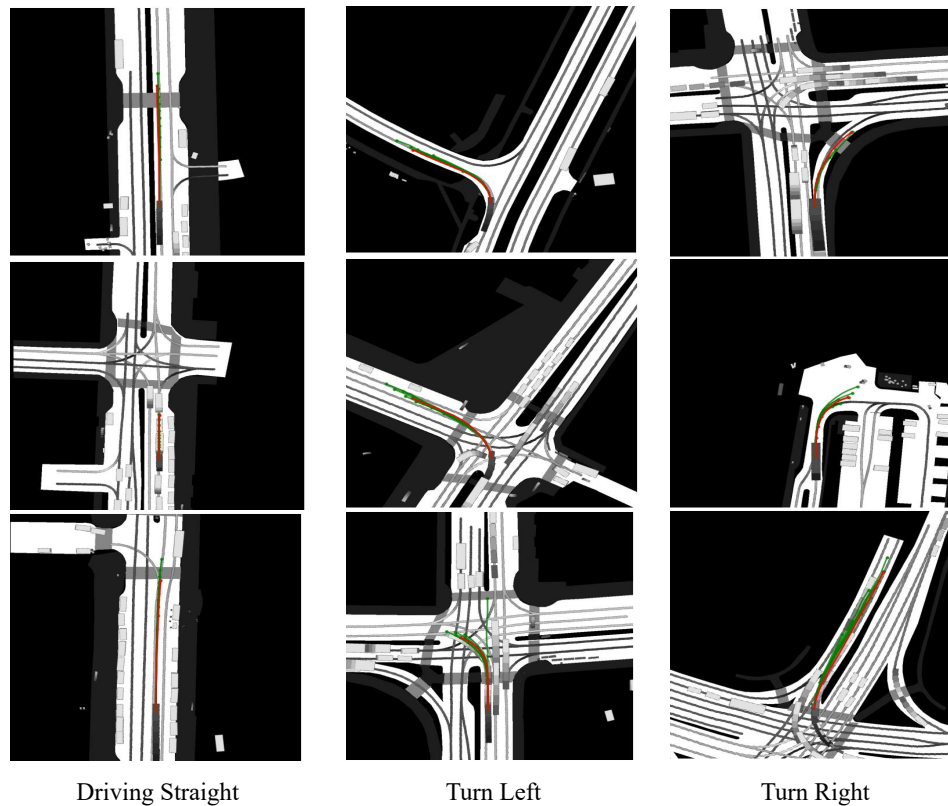


Fig. 6. Results of qualitative analysis on the NuScenes validation set. In this figure, a total of three different scenarios showing the prediction performance of our method are shown. (a) Straight ahead, (b) turn left, (c) turn right. The red lines denote our prediction results, and blue lines denote the ground truth.

- [5] W. Xiong, J. Chen, X. Zhang, Q. Wang, and Z. Qi, "Hierarchical attention network for planning-informed multi-agent trajectory prediction," in *2023 IEEE/RSJ International Conference on Intelligent Robots and Systems (IROS)*. IEEE, 2023, pp. 5501–5506.
- [6] Z. Zhou, L. Ye, J. Wang, K. Wu, and K. Lu, "Hivt: Hierarchical vector transformer for multi-agent motion prediction," in *Proceedings of the IEEE/CVF Conference on Computer Vision and Pattern Recognition*, 2022, pp. 8823–8833.
- [7] J. Gao, C. Sun, H. Zhao, Y. Shen, D. Anguelov, C. Li, and C. Schmid, "Vectornet: Encoding hd maps and agent dynamics from vectorized representation," in *Proceedings of the IEEE/CVF conference on computer vision and pattern recognition*, 2020, pp. 11 525–11 533.
- [8] H. Song, W. Ding, Y. Chen, S. Shen, M. Y. Wang, and Q. Chen, "Pip: Planning-informed trajectory prediction for autonomous driving," in *Computer Vision—ECCV 2020: 16th European Conference, Glasgow, UK, August 23–28, 2020, Proceedings, Part XXI 16*. Springer, 2020, pp. 598–614.
- [9] B. Varadarajan, A. Hefny, A. Srivastava, K. S. Refaat, N. Nayakanti, A. Cornman, K. Chen, B. Douillard, C. P. Lam, D. Anguelov *et al.*, "Multipath++: Efficient information fusion and trajectory aggregation for behavior prediction," in *2022 International Conference on Robotics and Automation (ICRA)*. IEEE, 2022, pp. 7814–7821.
- [10] H. Zhao, J. Gao, T. Lan, C. Sun, B. Sapp, B. Varadarajan, Y. Shen, Y. Shen, Y. Chai, C. Schmid *et al.*, "Tnt: Target-driven trajectory prediction," in *Conference on Robot Learning*. PMLR, 2021, pp. 895–904.
- [11] J. Gu, C. Sun, and H. Zhao, "Densentt: End-to-end trajectory prediction from dense goal sets," in *Proceedings of the IEEE/CVF International Conference on Computer Vision*, 2021, pp. 15 303–15 312.
- [12] G. Aydemir, A. K. Akan, and F. Güneş, "Adapt: Efficient multi-agent trajectory prediction with adaptation," in *Proceedings of the IEEE/CVF International Conference on Computer Vision*, 2023, pp. 8295–8305.
- [13] T. Gilles, S. Sabatini, D. Tsishkou, B. Stanciulescu, and F. Moutarde, "Gohome: Graph-oriented heatmap output for future motion estimation," in *2022 international conference on robotics and automation (ICRA)*. IEEE, 2022, pp. 9107–9114.
- [14] J. Wang, T. Ye, Z. Gu, and J. Chen, "Ltp: Lane-based trajectory prediction for autonomous driving," in *Proceedings of the IEEE/CVF Conference on Computer Vision and Pattern Recognition*, 2022, pp. 17 134–17 142.
- [15] A. Sadeghian, V. Kosaraju, A. Sadeghian, N. Hirose, H. Rezaatofghi, and S. Savarese, "Sophie: An attentive gan for predicting paths compliant to social and physical constraints," in *Proceedings of the IEEE/CVF conference on computer vision and pattern recognition*, 2019, pp. 1349–1358.
- [16] X. Li, X. Ying, and M. C. Chuah, "Grip++: Enhanced graph-based interaction-aware trajectory prediction for autonomous driving," *arXiv preprint arXiv:1907.07792*, 2019.
- [17] Y. Xu, L. Wang, Y. Wang, and Y. Fu, "Adaptive trajectory prediction via transferable gnn," in *Proceedings of the IEEE/CVF conference on computer vision and pattern recognition*, 2022, pp. 6520–6531.
- [18] L. Zhang, P. Li, S. Liu, and S. Shen, "Simpl: A simple and efficient multi-agent motion prediction baseline for autonomous driving," *IEEE Robotics and Automation Letters*, 2024.
- [19] X. Tang, M. Kan, S. Shan, Z. Ji, J. Bai, and X. Chen, "Hpnet: Dynamic trajectory forecasting with historical prediction attention," in *Proceedings of the IEEE/CVF Conference on Computer Vision and Pattern Recognition*, 2024, pp. 15 261–15 270.
- [20] X. Shi, X. Shao, Z. Fan, R. Jiang, H. Zhang, Z. Guo, G. Wu, W. Yuan, and R. Shibasaki, "Multimodal interaction-aware trajectory prediction in crowded space," in *Proceedings of the AAAI Conference on Artificial Intelligence*, vol. 34, no. 07, 2020, pp. 11 982–11 989.
- [21] C. Yang and Z. Pei, "Long-short term spatio-temporal aggregation for trajectory prediction," *IEEE Transactions on Intelligent Transportation Systems*, vol. 24, no. 4, pp. 4114–4126, 2023.
- [22] X. Zhou, X. Chen, and J. Yang, "Edge-enhanced heterogeneous graph transformer with priority-based feature aggregation for multi-agent trajectory prediction," *IEEE Transactions on Intelligent Transportation Systems*, 2024.
- [23] A. Mohamed, K. Qian, M. Elhoseiny, and C. Claudel, "Social-stgenn: A social spatio-temporal graph convolutional neural network for human trajectory prediction," in *Proceedings of the IEEE/CVF conference on computer vision and pattern recognition*, 2020, pp. 14 424–14 432.
- [24] T. Salzmann, B. Ivanovic, P. Chakravarty, and M. Pavone, "Trajectron++:

- Dynamically-feasible trajectory forecasting with heterogeneous data,” in *Computer Vision—ECCV 2020: 16th European Conference, Glasgow, UK, August 23–28, 2020, Proceedings, Part XVIII 16*. Springer, 2020, pp. 683–700.
- [25] X. Jia, P. Wu, L. Chen, Y. Liu, H. Li, and J. Yan, “Hdgt: Heterogeneous driving graph transformer for multi-agent trajectory prediction via scene encoding,” *IEEE transactions on pattern analysis and machine intelligence*, 2023.
- [26] T. Zhang, M. Fu, Y. Yang, W. Song, and T. Liu, “Edge-enriched graph transformer for multi-agent trajectory prediction with relative positional semantics,” *IEEE Transactions on Instrumentation and Measurement*, 2024.
- [27] S. Shi, L. Jiang, D. Dai, and B. Schiele, “Motion transformer with global intention localization and local movement refinement,” *Advances in Neural Information Processing Systems*, vol. 35, pp. 6531–6543, 2022.
- [28] N. Deo, E. Wolff, and O. Beijbom, “Multimodal trajectory prediction conditioned on lane-graph traversals,” in *Conference on Robot Learning*. PMLR, 2022, pp. 203–212.
- [29] L. Li, X. Wang, J. Lian, J. Zhao, and J. Hu, “Efficient vehicle trajectory prediction with goal lane segments and dual-stream cross attention,” *IEEE Transactions on Intelligent Transportation Systems*, 2024.
- [30] M. Liang, B. Yang, R. Hu, Y. Chen, R. Liao, S. Feng, and R. Urtasun, “Learning lane graph representations for motion forecasting,” in *Computer Vision—ECCV 2020: 16th European Conference, Glasgow, UK, August 23–28, 2020, Proceedings, Part II 16*. Springer, 2020, pp. 541–556.
- [31] B. Zhang, N. Song, and L. Zhang, “Decoupling motion forecasting into directional intentions and dynamic states,” *arXiv preprint arXiv:2410.05982*, 2024.
- [32] X. Mo, H. Liu, Z. Huang, X. Li, and C. Lv, “Map-adaptive multimodal trajectory prediction via intention-aware unimodal trajectory predictors,” *IEEE Transactions on Intelligent Transportation Systems*, 2023.
- [33] H. Caesar, V. Bankiti, A. H. Lang, S. Vora, V. E. Liong, Q. Xu, A. Krishnan, Y. Pan, G. Baldan, and O. Beijbom, “nusenes: A multimodal dataset for autonomous driving,” in *Proceedings of the IEEE/CVF conference on computer vision and pattern recognition*, 2020, pp. 11 621–11 631.
- [34] M.-F. Chang, J. Lambert, P. Sangkloy, J. Singh, S. Bak, A. Hartnett, D. Wang, P. Carr, S. Lucey, D. Ramanan *et al.*, “Argoverse: 3d tracking and forecasting with rich maps,” in *Proceedings of the IEEE/CVF conference on computer vision and pattern recognition*, 2019, pp. 8748–8757.
- [35] T. Phan-Minh, E. C. Grigore, F. A. Boulton, O. Beijbom, and E. M. Wolff, “Covernet: Multimodal behavior prediction using trajectory sets,” in *Proceedings of the IEEE/CVF conference on computer vision and pattern recognition*, 2020, pp. 14 074–14 083.
- [36] T. Salzmann, B. Ivanovic, P. Chakravarty, and M. Pavone, “Trajectron++: Dynamically-feasible trajectory forecasting with heterogeneous data,” in *Computer Vision—ECCV 2020: 16th European Conference, Glasgow, UK, August 23–28, 2020, Proceedings, Part XVIII 16*. Springer, 2020, pp. 683–700.
- [37] R. Girgis, F. Golemo, F. Codevilla, M. Weiss, J. A. D’Souza, S. E. Kahou, F. Heide, and C. Pal, “Latent variable sequential set transformers for joint multi-agent motion prediction,” *arXiv preprint arXiv:2104.00563*, 2021.
- [38] P. Xu, J.-B. Hayet, and I. Karamouzas, “Context-aware timewise vaes for real-time vehicle trajectory prediction,” *IEEE Robotics and Automation Letters*, 2023.
- [39] B. Kim, S. H. Park, S. Lee, E. Khoshimjonov, D. Kum, J. Kim, J. S. Kim, and J. W. Choi, “Lapred: Lane-aware prediction of multi-modal future trajectories of dynamic agents,” in *Proceedings of the IEEE/CVF Conference on Computer Vision and Pattern Recognition*, 2021, pp. 14 636–14 645.
- [40] T. Gilles, S. Sabatini, D. Tsishkou, B. Stanculescu, and F. Moutarde, “Thomas: Trajectory heatmap output with learned multi-agent sampling,” *arXiv preprint arXiv:2110.06607*, 2021.
- [41] Z. Zhang, Z. Hua, M. Chen, W. Lu, B. Lin, D. Cai, and W. Wang, “G2ltraj: A global-to-local generation approach for trajectory prediction,” *arXiv preprint arXiv:2404.19330*, 2024.
- [42] J. Ngiam, B. Caine, V. Vasudevan, Z. Zhang, H.-T. L. Chiang, J. Ling, R. Roelofs, A. Bewley, C. Liu, A. Venugopal *et al.*, “Scene transformer: A unified architecture for predicting multiple agent trajectories,” *arXiv preprint arXiv:2106.08417*, 2021.
- [43] J. Chen, Z. Wang, J. Wang, and B. Cai, “Q-eonet: Implicit social modeling for trajectory prediction via experience-anchored queries,” *IET Intelligent Transport Systems*, vol. 18, no. 6, pp. 1004–1015, 2024.
- [44] S. Afshar, N. Deo, A. Bhagat, T. Chakraborty, Y. Shao, B. R. Budharaju, A. Deshpande, and H. C. Motion, “Pbp: Path-based trajectory prediction for autonomous driving,” in *2024 IEEE International Conference on Robotics and Automation (ICRA)*. IEEE, 2024, pp. 12 927–12 934.



**Wenyi Xiong** received his B.E. degree in mechanical and electrical engineering from Central South University, Changsha, China, in 2021. He is currently working toward the Ph.D. degree in the College of Mechanical Engineering, Zhejiang University, Hangzhou, China.

His research interests include vehicle motion prediction, trajectory planning, and deep learning.



**Jian Chen** (Senior Member, IEEE) received the B.E. and M.E. degrees from Zhejiang University, Hangzhou, China, in 1998 and 2001, respectively, and the Ph.D. degree in electrical engineering from Clemson University, Clemson, SC, USA, in 2005. He was a Research Fellow with the University of Michigan, Ann Arbor, MI, USA, from 2006 to 2008, where he was involved in fuel cell modeling and control. From 2013 to 2024, he was a professor in the College of Control Science and Engineering, Zhejiang University. Currently, he is a professor in

the School of Automation and Intelligent Manufacturing, Southern University of Science and Technology, Shenzhen, China. His research interests include modeling and control of fuel cell systems, visual servo techniques, battery management systems, and applied nonlinear control.



**Qi Ziheng** received his Bachelor’s degree in 2019 and master degree in 2022, both from the College of Control Science and Engineering, Zhejiang University.

His research interests include vehicle dynamics, path planning, and tracking of autonomous vehicles.